creative commons
COMMONS DEED

저작자표시-비영리-동일조건변경허락 2.0 대한민국

이용자는 아래의 조건을 따르는 경우에 한하여 자유롭게

- 이 저작물을 복제, 배포, 전송, 전시, 공연 및 방송할 수 있습니다.
- 이차적 저작물을 작성할 수 있습니다.

다음과 같은 조건을 따라야 합니다:

저작자표시. 귀하는 원저작자를 표시하여야 합니다.

비영리. 귀하는 이 저작물을 영리 목적으로 이용할 수 없습니다.

동일조건변경허락. 귀하가 이 저작물을 개작, 변형 또는 가공했을 경우에는, 이 저작물과 동일한 이용허락조건하에서만 배포할 수 있습니다.

- 귀하는, 이 저작물의 재이용이나 배포의 경우, 이 저작물에 적용된 이용허락조건을 명확하게 나타내어야 합니다.
- 저작권자로부터 별도의 허가를 받으면 이러한 조건들은 적용되지 않습니다.

저작권법에 따른 이용자의 권리는 위의 내용에 의하여 영향을 받지 않습니다.

이것은 이용허락규약(Legal Code)을 이해하기 쉽게 요약한 것입니다.

Disclaimer

dCollection

치의학박사학위논문

Axial displacement of abutments in implants with internal tapered connection after cyclic loading: Linear mixed model analysis

내측연결형 임플란트에서 반복하중에 따른 지대주의 수직침하현상: 선형혼합모형 분석

2014 년 2 월

서울대학교 대학원

치의과학과 치과보철학 전공

설 현 우

Axial displacement of abutments in implants with internal tapered connection after cyclic loading: Linear mixed model analysis

지도교수 허 성 주

이 논문을 치의학박사 학위논문으로 제출함

2013 년 10 월

서울대학교 대학원

치의과학과 치과보철학 전공

설 현 우

설현우의 치의학박사 학위논문을 인준함

2013 년 12 월

위 원 장 (인)

부위원장 (인)

위 원 (인)

위 원 (인)

위 원 (인)

-ABSTRACT-

Axial displacement of abutments in implants with internal tapered connection after cyclic loading: Linear mixed model analysis

Hyon-Woo Seol, D.D.S., M.S.D.

Department of Prosthodontics, Graduate School, Seoul National University

*(Directed by Professor **Seong-Joo Heo**, D.D.S., M.S., Ph.D.)*

Purpose: The purpose of this study was to analyze the patterns of the axial displacement of implant-abutment assembly after cyclic loading, and to figure out the plateau in the amount of axial displacement in internal tapered connection.

Materials and methods: External butt-joint connection implant and internal tapered connection implant were connected with three types of abutment for cement-retained prostheses. Three groups of external type abutment (Ext group), internal tapered one-piece type abutment (Int-1 group), and internal tapered two-piece type abutment (Int-2 group) were prepared. For each group, 7 implants and

abutments were tested. The implant-abutments assemblies were clamped into the implant holder for vertical loads. A dynamic cyclic loading was applied for 150 N at a frequency of 3 Hz. The amount of axial displacement after tightening was measured before cyclic loading, and the Periotest® values (PTVs) and removal torque values (RTVs) were measured for each group before and after the cyclic loading. The amount of axial displacement of the abutment into the implant was measured at each cycle of 0, 10, 100, 1,000, 10,000, 100,000, 500,000, and 1,000,000. A repeated measures analysis of variance (ANOVA) for the overall effect of cyclic loading. Thereafter, the pattern analysis by linear mixed model were used for statistical analysis of longitudinal data. Differences at $P < 0.05$ were considered statistically significant. Microscopic computed tomography (micro-CT) was used to evaluate the internal structure, and scanning electronic microscopy (SEM) was used to evaluate the surface of implant-abutment connection.

Results: The mean axial displacement after tightening were 4.0 ± 1.41 μm in Ext group, 31.1 ± 9.48 μm in Int-1 group, and 48.3 ± 8.44 μm in Int-2 group. Before the cyclic loading, the PTVs were not different in each group. After the cycles, the PTV decreased in Int-2 group. The RTV in Int-1 group showed significantly higher value before the cyclic loading. After the cycles, each group showed significant decrease in RTV values, and Int-2 group showed the lowest RTV value.

The mean axial displacement after 1 million cycles were 0.6 ± 0.54 μm in Ext group, 3.7 ± 0.76 μm in Int-1 group, and 9.0 ± 2.38 μm in Int-2 group. In the pattern analysis, the breakpoint was found at 171 cycles. There were no declining pattern of axial displacement for the Ext group and the after of the breakpoint (171 cycles) of Int-1 group. However, Int-2 group showed continuous axial displacement. In the SEM evaluation, the surface wear were found in all groups.

Conclusions: Within the limitations of this study, the following conclusions can be drawn:

1. The axial displacements according to the tightening torque occurred in all groups.
2. The surface wear of the implant-abutment connection after cyclic loading were noticed in all groups.
3. The periotest values remained stable, but the removal torque value decreased after cyclic loading in all groups.
4. In the analysis by linear mixed model, Ext and Int-1 group showed the plateau of axial displacement at early phase of cyclic loading. The exact point of plateau was hardly figured out in Int-2 group, but the rate of axial displacement slowed after 100,000 cycles.

This study demonstrated the patterns of axial displacement in internal implant system and the decrease in removal torque value. In the clinical aspect, it is

recommended that the screw be retightened after at least one month to minimize the screw loosening and clinical prosthetic errors.

Keywords : axial displacement, linear mixed model, settling effect, cyclic loading, internal tapered connection, dental implant-abutment design

Student number : 2010-31197

Axial displacement of abutments in implants with internal tapered connection after cyclic loading: Linear mixed model analysis

Hyon-Woo Seol, D.D.S., M.S.D.

Department of Prosthodontics, Graduate School, Seoul National University

*(Directed by Professor **Seong-Joo Heo**, D.D.S., M.S., Ph.D.)*

CONTENTS

I. INTRODUCTION

Dental implants have become one of the most reliable and predictable rehabilitation treatment in partially or fully edentulous patient, so dental implants have been used extensively by clinicians. Dental implant has shown satisfactory long-term results with high success rate above 90%.[1-3] Despite these favorable success rates, recent studies have reported implant complications, including screw loosening, fracture, and implant fractures.[4-6]

The most frequent complications of the implant with external connection is the loosening of the abutment screw.[7] To overcome the joint instability between external implant and abutment connection, internal tapered connection types have been introduced, and become widely spread.[8, 9] The internal connection design resulted in favorable mechanical stability in comparison with external connection design. Several studies have reported superior joint stability of internal tapered connection than external butt-joint connection.[10-12] Internal tapered connection showed better resistance to the bending force[13] and lower incidence of mechanical complications in comparison with the external butt-joint connection type.[14, 15] In addition, several studies reported that the internal tapered connection showed low level of bacterial leakage, which might be one of the risk factor for peri-implantitis and marginal bone loss.[16-19] In this regard, internal connection has become popular for its mechanical and biological advantages over external connection.

In spite of the superior joint stability than external connection, there is increasing concern about the axial displacement of abutment into the implant with internal tapered connection. For implants with internal tapered connection, certain amount of axial displacement occurs during abutment tightening.[20-23] Accordingly, many researches have focused on the axial displacement of implant-abutment assembly.

The settling phenomenon (embedment relaxation) occurs when small irregularities on the screw interface wear, so that the tension in the screw decreases and the screw is more easily loosened by functional forces.[24] Even more, it has been shown that preload decreases over time in implant screws, even when external forces are not applied to the system.[25] Therefore, repeated tightening, at least twice, have been recommended to minimize the settling effect during the connection of abutment into implant.[26-30]

In a recent study about implant-abutment connection after cyclic loading, the axial displacements were observed both in external and internal implant after one million cycles.[31] However, the study simulated the laboratory procedure with implant replica. Since the discrepancy of axial displacement was observed between the implant and the implant replica groups,[23] therefore, the implant-abutment assembly would be more appropriate for simulating the oral condition.

Up to date, researches have mainly focused on the amount of axial displacement according to the tightening torque,[23, 28] or on comparing the value in before and after the cyclic loading.[31] In this regard, many clinicians let the abutment displace

axially with provisional prostheses for a while. However, there are few clinical guide to the time period that the settling fully occurs.

In the mechanical analysis of internal tapered interference fit,[20-22] the axial location of internally tapered connection would converge on the certain extent. So, the axial displacement of abutment could be speculated to converge to a specific value.

The aim of this study, therefore, was to analyze the patterns of the axial displacement of implant-abutment assembly after cyclic loading in internal tapered connection system, and to figure out the plateau in the amount of axial displacement in internal tapered connection.

II. MATERIALS AND METHODS

1. Implants and abutments

The implants and abutments from Warantec Co. (Seoul, Korea) were prepared for this study. External type implant (Hexplant® ø4.3 x 13mm, Art.No. FHT43130) and internal type implant (Inplant® ø4.3 x 13mm, Art.No. FIT43130) were used (Table I and Fig. 1). Hexplant® has an external hex at the prospective connection with abutment, and Inplant® has an internal octagonal connection between the implant and abutment. The implant-abutment interfaces were external butt joint and 7 degree tapered internal connection, respectively. The mechanical properties and parameters of the implant systems are described in Table II and III.

Table I. Implant and abutment systems used in this study (7 samples per group)

Group	Implant system, diameter	Art No.	Abutment	Art No.
Ext	Hexplant® 4.3mm	FHT43130	Straight Abutment® (ø4.3, GH 2.0, AH 6.0)	H0SA4326H
Int-1	Inplant® 4.3mm	FIT43130	Top Abutment® (Non-Oct ø4.5, GH 2.0, AH 6.0)	I0TA4526
Int-2	Inplant® 4.3mm	FIT43130	Top Abutment® (Oct ø4.5, GH 2.0, AH 6.0)	I0TA4526E

Table II. Mechanical properties utilized for the study

Material	Composition	Elastic modulus
Implant	Titanium grade 4	105 GPa
Abutment	Titanium Ti-6Al-4V (grade 5)	113.8 GPa

Table III. Parameters of the tapered connection of internal implant system utilized for the study

	Group	
	Int-1	Int-2
Maximum length of contact	2.5 mm	1.6 mm
Taper angle	7°	7°

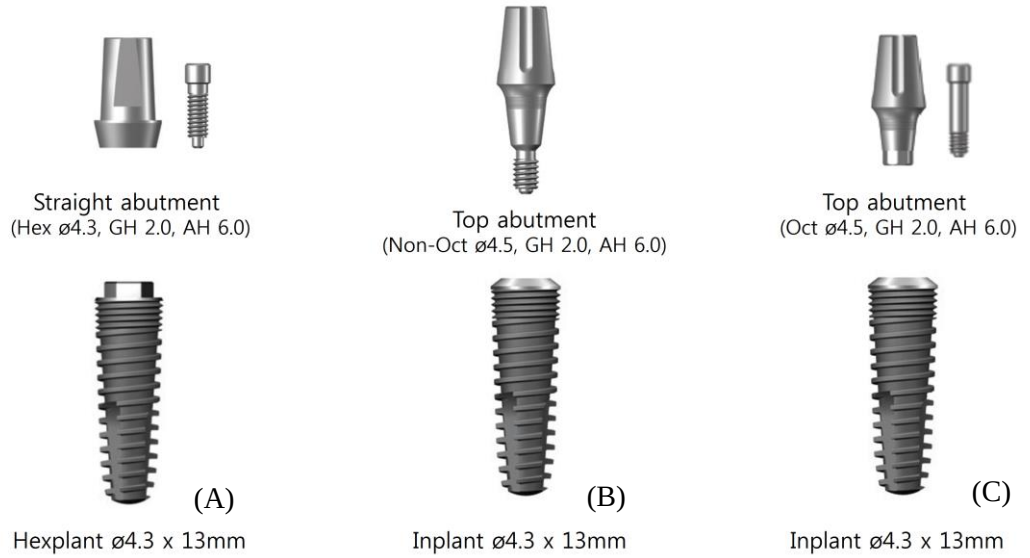

Fig. 1. This picture shows three groups of implant-abutment assemblies. **A**: Ext group (left): Straight abutment® was connected to Hexplant® implant; **B**: Int-1 group (center): one-piece Top abutment® (non-octagonal) was connected to Inplant® implant; **C**: Int-2 group (right): two-piece Top abutment® (octagonal) was connected to Inplant® implant.

Three types of abutment for cement-retained prostheses were used in this study. Straight Abutment® (ø4.3, gingival height 2.0mm, abutment height 6.0mm Art.No. H0SA4326H) was used for external type implant (Ext group) (Fig. 1A). Top Abutment® of one-piece type (non-octagonal, ø4.5, gingival height 2.0mm, abutment height 6.0mm Art.No. I0TA4526) and Top Abutment® of two-piece type

(octagonal, ø4.5, gingival height 2.0mm, abutment height 6.0mm Art.No. I0TA4526E) were used for internal type implant, respectively (Int-1 and Int-2 group) (Fig 1B and Fig. 1C).

For each group, seven implants and abutments were prepared, and each assembly was clamped in an implant holder (Fig. 2B).

2. Cyclic loading apparatus

The custom-made cyclic loading machine (Hatis Co., Hwaseong, Korea) was used to reproduce human chewing simulation (Fig.2A). As the pear-shaped cam rotates, the vertical reciprocal movement of impact rod applies chewing-like cyclic loads to the specimens.[32]

The specimens were clamped into implant holder composed of collet and nut (Nikken, Japan) (Fig. 2B) by using torque wrench (230DB3, Tohnichi, Japan) in 300 N·cm and this assembly was connected to the stainless steel holder. The assembly was fixed to the holder along the long axis of implant for vertical loads. The vertical loads would have a definitive effect on the axial displacement of the abutment to the implant. A hemispherical metal cap made of stainless steel was manufactured and seated onto the unmodified abutments according to the ISO 14801 (Fig. 2B). The metal cap was intended to mimic the crown and to prevent the deformation of abutment from the impact rod.

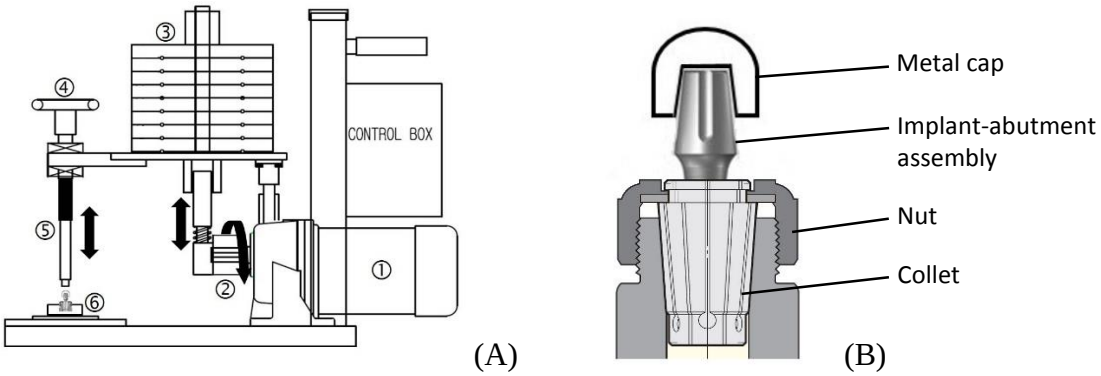

Fig. 2. Custom-made cyclic loading apparatus. **A**: Cyclic loading machine, ①: motor, ②: cam, ③: weight, ④: height adjusting screw ⑤: impact rod, ⑥: implant holder. **B**: Implant-abutment assembly was clamped into implant holder (collet and nut)

According to the instructions for user from the manufacturer, tightening torque of 30 Ncm was applied. Each implant and abutment was connected and the torque was applied twice at a 10 minute interval using a digital torque gauge (MGT50, Mark-10 Co., Hicksville, NY, USA) (Fig. 3).

Fig. 3. Digital torque gauge was used to tighten the abutment into implant at desired torque.

3. Setting the applied load

According to whole height (h_1) from the metal hemispherical cap to the base of implant holder, the prop for load cell was adjusted that the height (h_2) of the load cell to be same with h_1. *i.e.*, $h_1 = h_2$. (Fig. 4)

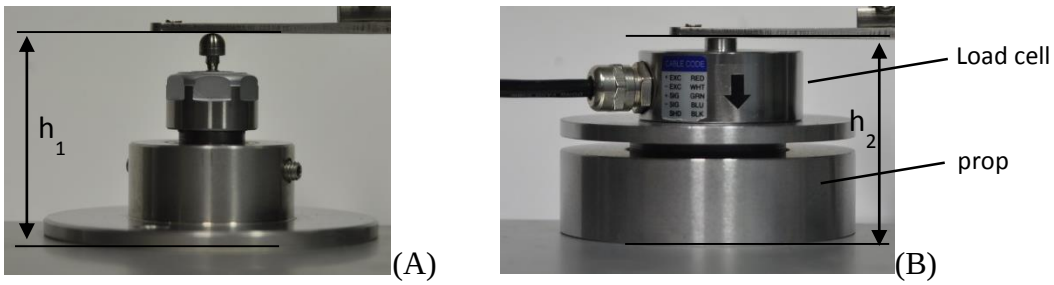

(A) (B)

Fig. 4. Setting the applied load with a load cell. **A**: Height from metal cap to base of implant holder (h_1) was measured for each implant-abutment assembly. **B**: The prop was adjusted for the load cell to be the same height (h_1=h_2).

Each applied load was calibrated with a load cell (MNC-500L, CAS Korea, Seoul, Korea) and strain analysis program (STT-200P, CAS Korea, Seoul, Korea). The load of 150 N, which is within the physiologic clinical range,[33, 34] were set to be applied by adjusting the height of impact rod position. In all experiments, loads of 150 N at a frequency of 3 Hz were applied. The dynamic cyclic loads were confirmed by monitoring the strain analysis program (Fig. 5).

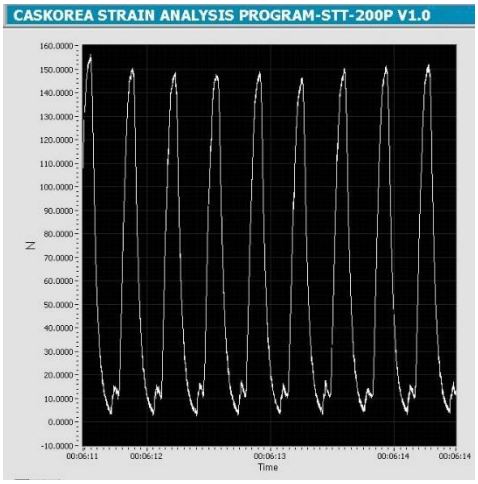

Fig. 5. Monitoring the applied load using strain analysis program.

4. Measuring the length of implant-abutment assembly

The total length of implant-abutment assemblies were measured using an electronic digital micrometer (No. 293-240, Mitutoyo, Kawasaki, Japan), which was held in a vise (Fig. 6). The measurements were made by the same operator and were accurate up to 0.001 mm (1 μm). The amount of axial displacement of the abutment into the implant was calculated by comparing the total length of specimen at each measuring time (Fig. 7).


(A)
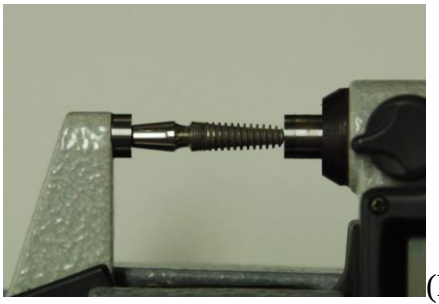
(B)

Fig. 6. Implant-abutment assembly in the electronic digital micrometer. **A**: Overall view and **B**: magnified view of measurement of implant-abutment assembly.

The schematic diagram of the overall sequence of the test is shown in Fig. 7.

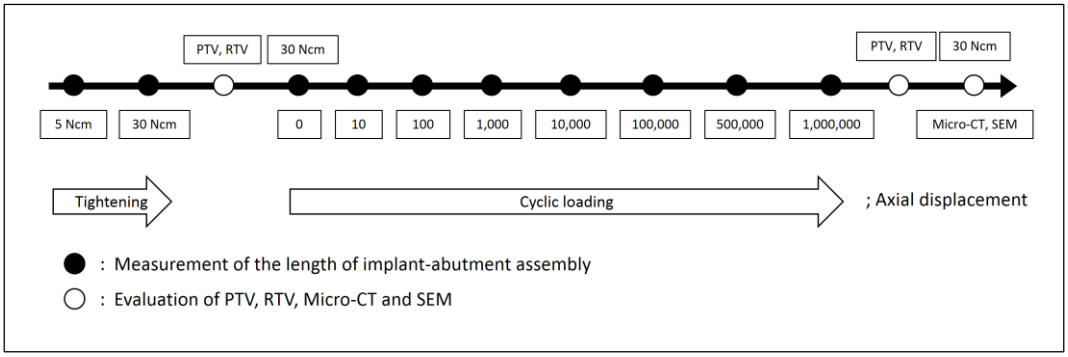

Fig. 7. Schematic diagram of sequence of test. The total length of each specimen was measured at each time marked in black circle. Throughout the study, 30 Ncm tightening torque was applied repeatedly at 10 minutes interval.

5. Axial displacement in tightening

The amount of axial displacement due to the tightening torque was measured at 5 Ncm and 30 Ncm, respectively. The initial length of implant-abutment assembly at 5 Ncm tightening was set as a baseline for each sample,[28] and the changes in the length of each implant-abutment assembly after 30 Ncm repeated tightening were calculated for axial displacement.

6. Periotest value and removal torque value measurement before the cyclic loading

Prior to the cyclic loading, the Periotest value (PTV) was measured (Periotest device, Model No.3218, Medizintechnik Gulden, Modautal, Germany). A point was marked at 2mm from the most coronal point of the abutment to measure the PTV.

Two minutes after the repeated tightening at 30 Ncm, the removal torque value

(RTV) was measured for each specimen using a digital torque gauge before the cyclic loading.

7. Axial displacement in cyclic loading

After PTVs and RTVs were measured, the initial length of implant-abutment assemblies were measured after 30 Ncm tightening torque was applied twice at a 10 minute interval. According to the previous study,[31] most of the amount of axial displacement occurred in early phase of cyclic loading. Therefore, the measurement of total length of implant-abutment assemblies were conducted at exponential cycles in 10^n, that is, at each cycle of 0, 10, 100, 1,000, 10,000, 100,000, 500,000, and 1,000,000.

8. Periotest value and removal torque value measurement after the cyclic loading

After the one million cyclic loads, PTVs were measured again. The RTVs were also measured again for each specimen using a digital torque gauge.

9. Microscopic computed tomography

The microscopic computed tomography (micro-CT) was used to evaluate the internal structure for each group. The micro-CT provide 3-dimensional structure images without sacrificing the specimen. Three specimens were chosen at random

from each group (one sample per group). For each specimen, repeated tightening of 30 Ncm was applied again. The internal structures of the specimens were analyzed with the micro-CT (SkyScan1173, SKYSCAN, Kartuizersweg, Kontich, Belgium) with X-ray source with 130 kV and 60 μA, and with the image pixel size of 5.33 μm. The number of rows and columns was 2240, and the rotation step was 0.300 degree. A 1.0 mm aluminum filter was used, and the exposure time was 500 ms.

10. Scanning electron microscope analysis

The surface characteristics of implant-abutment connection site were examined with a scanning electronic microscopy (SEM). Three specimens used in micro-CT evaluation were sectioned and rinsed with tap water, soaked in an ultrasonic ethanol bath (Saehan Cleaner, Saehan Ultrasonic Co., Seoul, Korea) for 10 minutes, and then dried with compressed air. The specimens were coated with platinum in a sputter coater unit and were introduced into the vacuum chamber of a field emission scanning electron microscope (FE-SEM, S-4700, HITACHI, Tokyo, Japan) with an accelerating voltage of 15kV and were observed with ×35, ×100, and ×500 magnification.

11. Statistical analysis

Statistical analysis was performed using SPSS 21 (IBM® SPSS® Statistics, IBM Co., NY, USA). Repeated measures analysis of variance (ANOVA) for the overall

effect of cyclic loading to the axial displacement of implant-abutment assemblies, and the independent samples T-test for *post hoc* comparison were conducted. Differences at $P < 0.05$ were considered statistically significant.

Kruskal-Wallis tests and Mann-Whitney tests were employed to compare the PTVs and RTVs between groups at the time of before the cyclic loading and after the cyclic loading.

Wilcoxon signed rank test was used to compare the value of before and after the cyclic loads of PTVs and RTVs for each group.

The patterns of axial displacement according to the cyclic loading in each group were analyzed using R Statistics version 3.0.1 (R foundation for Statistical Computing, Vienna, Austria)[35] with package lme4: Linear mixed-effects models.[36] This model is particularly useful in settings where repeated measurements are made on the same specimen over time. The repeated measurement on each specimen (21 subject, 7 samples × 3 groups) have a within-subject correlation. That is, the repeatedly measured data (longitudinal data) from the same subject cannot be regarded as independent from each other, therefore, the analysis for the longitudinal data should allow correlation between the observations.[37, 38] The mixed model analysis provides a flexible approach in these situation by adding the random effect to the fixed effect. This allows us to resolve the non-independence by assuming a different random intercepts (*i.e.*, different baseline value of axial displacement) for each subject.[39]

In this study, the mean responses at each cycle were transformed to common logarithmic scale for convenience in calculation, and were fitted to the linear mixed models. Thereafter, the formula for this model was determined, and the patterns of axial displacement were figured out.

III. RESULTS

1. Axial displacement in tightening

The initial length of specimens were measured at 5 Ncm tightening.[28] The mean axial displacements of the abutment into the implant after 30 Ncm tightening from baseline of 5 Ncm are shown in Table IV and Fig. 8. There was significantly more axial displacement in the Int-1 and Int-2 group than in the Ext group.

Table IV. Mean (SD) axial displacement of implant-abutment assemblies after 30 Ncm tightening (μm)

Tightening	Group		
	Ext	Int-1	Int-2
5 Ncm	0 (0)	0 (0)	0 (0)
30 Ncm	-4.0 (1.41)	-31.1 (9.48)	-48.3 (8.44)

SD: standard deviation; Ext: External type implant; Int-1: Internal type implant with one-piece abutment; Int-2: Internal type implant with two-piece abutment.

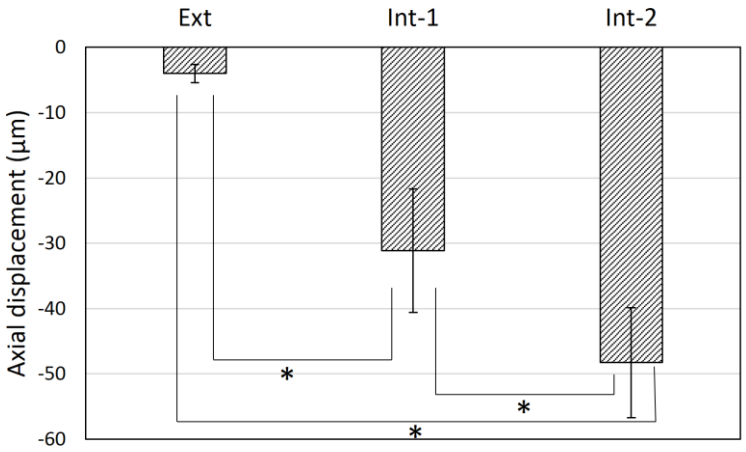

Fig. 8. The amount of axial displacement after 30 Ncm tightening. Each group showed significant difference ($P < 0.01$).

2. PTVs and RTVs of before and after the one million cyclic loading

The mean PTVs and RTVs are shown in Table V and VI. The comparison between groups in PTV showed that there were no statistically different in between the before the cyclic loads, however the PTV in Int-2 group after the cyclic loads showed significant difference. In the Ext and Int-1 group, there were no statistically significant difference between before and after the cyclic loads, however the Int-2 group showed decreased PTV after cyclic loads (Table V and Fig. 9).

Table V. Mean (SD) Periotest value of before and after cyclic loading

	Ext		Int-1		Int-2	
	Before	After	Before	After	Before	After
PTV	-7.8 (0.29)	-7.6 (0.28)	-7.7 (0.40)	-7.5 (0.46)	-7.6 (0.39)	-6.7† (0.26)

† designate significantly different between "After" groups.

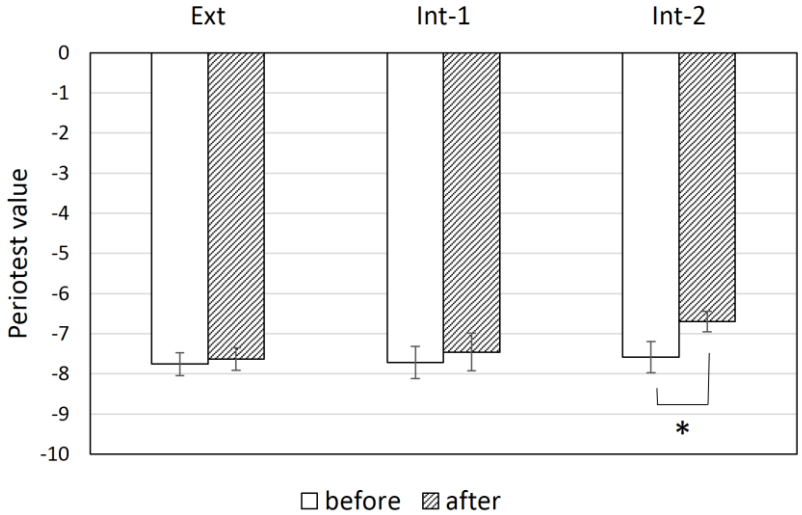

Fig. 9. Periotest values measured before and after the cyclic loading are shown. Periotest value in comparison of before with after the cyclic loading in Int-2 group showed significant difference ($P < 0.01$).

In the comparison of RTV between groups, the Int-1 group showed statistically significantly higher RTV before the cyclic loads, and the Int-2 group showed statistically significantly lower RTV after the cyclic loads (Table VI and Fig.10). The percentage of removal torque compared to tightening torque of 30 Ncm, 114.2% was recorded in the Before of Int-1 group, while other group showed about 101%. For all group, the RTVs decreased after cyclic loads. The percentage of removal torque was 52.1% in the After of Int-2 group, while other group showed about 75%.

Table VI. Mean (SD) removal torque value of before and after cyclic loading (Ncm)

	Ext		Int-1		Int-2	
	Before	After	Before	After	Before	After
RTV	30.6 (1.84)	22.1 (2.91)	34.3¶ (2.64)	23.4 (3.52)	30.4 (1.31)	15.6§ (4.81)

Different symbols (¶ and §) designate significantly different groups "Before" and "After", respectively.

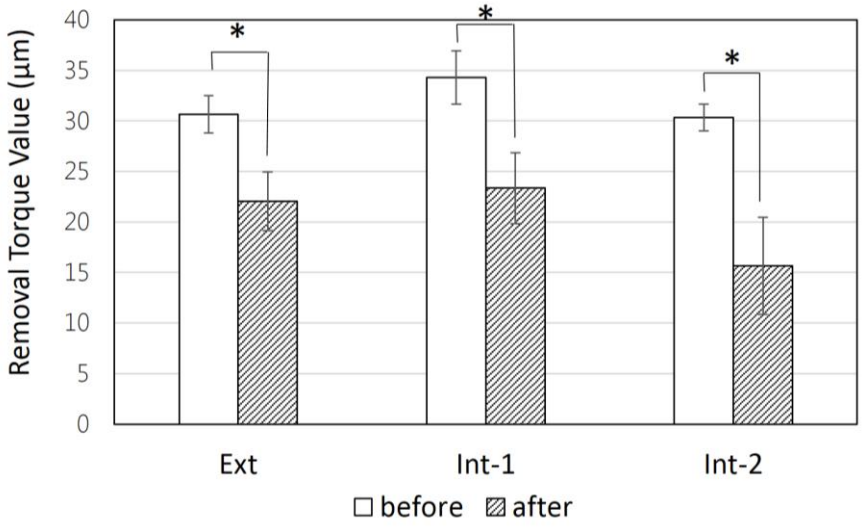

Fig. 10. Removal torque value of each group. The RTVs decreased in all groups ($P < 0.01$).

3. Axial displacement during cyclic loading

The mean axial displacement of implant-abutment assemblies at each cycle are shown in Table VII and Fig. 11.

Table VII. Mean (SD) axial displacement of abutment at each cycle (μm)

Cycles	Group		
	Ext	Int-1	Int-2
0	0 (0)	0 (0)	0 (0)
10	-0.1 (0.39)	-1.6 (0.79)	-2.7 (1.80)
100	-0.6 (0.54)	-3.3 (0.76)	-4.7 (1.80)
1,000	-0.7 (0.49)	-3.6 (0.98)	-6.0 (2.00)
10,000	-0.7 (0.49)	-3.3 (0.76)	-7.3 (1.70)
100,000	-0.7 (0.49)	-3.4 (0.79)	-8.3 (1.89)
500,000	-0.7 (0.49)	-3.6 (0.54)	-8.7 (1.70)
1,000,000	-0.6 (0.54)	-3.7 (0.76)	-9.0 (2.38)

Ext: External type implant; Int-1: Internal type implant with one-piece abutment; Int-2 : Internal type implant with two-piece abutment.

The amount of axial displacement at 1,000,000 cycles of Ext group decreased -0.1 μm compared with the prior cycles. However, the value was within the error range, therefore it could be neglected.

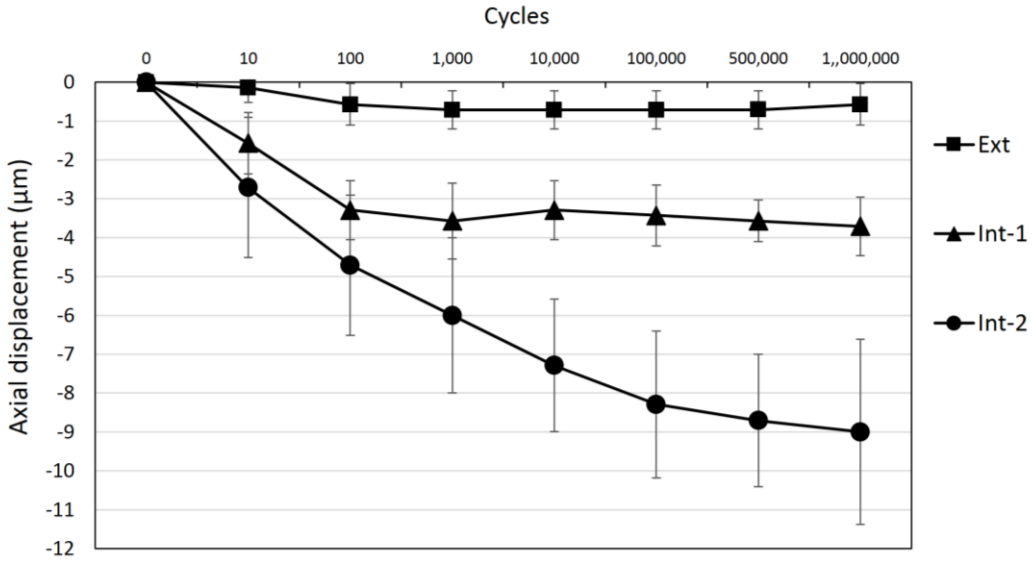

Fig. 11. Axial displacement during cyclic loading.

Mauchly's test indicated that the assumption of sphericity had been violated (χ^2=105.154, P < 0.0001), therefore multivariate tests were used. The results revealed that the changes of axial displacement value showed statistically significant difference between groups (P < 0.05).

An independent samples T-test was performed for each group at corrected significance level by Bonferroni's method for *post hoc* comparison.

A significant difference was found at each cycle between Ext and Int-1 group. Also, significant difference was found between Ext and Int-2 group at each cycle except cycle at 10th. However, for internal tapered implant-abutment group (Int-1 vs. Int-2), significant difference was found only after 10,000 cycles. Statistically significant difference was not found between Int-1 and Int-2 until 1,000 cycles.

4. The pattern analysis by linear mixed model

The patterns of axial displacement for each group were analyzed by linear mixed models in the R Statistics with package lme4.

The individual observations of each 21 subject are represented in thin lines (Fig. 12-1). To visualize the patterns of each group, the mean response curve was induced by calculating the mean at each cyclic loading. In the mean response curve, at a glance, significant declining patterns at earlier phase and gradual declining patterns at latter phase were found in each group as thick lines (Fig. 12-2).

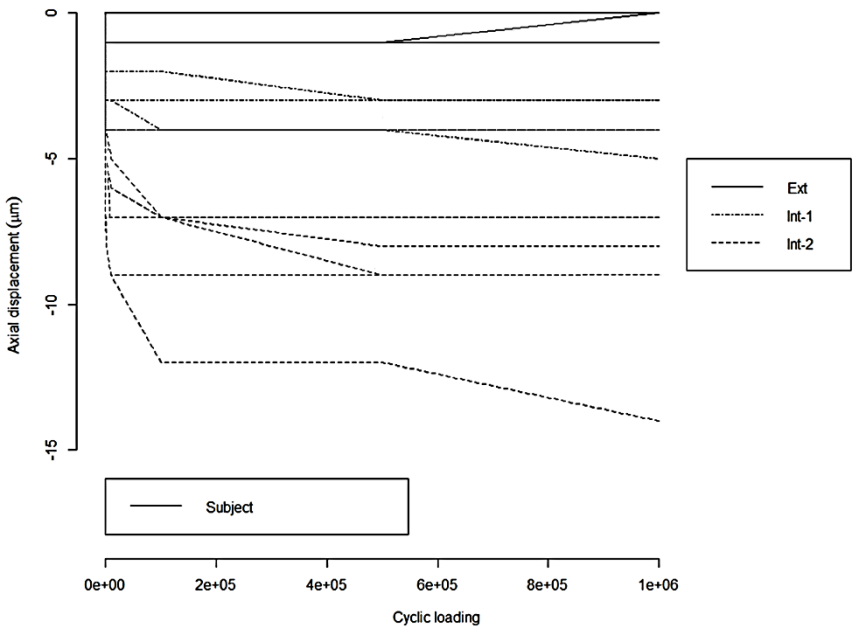

Fig. 12-1. The individual observations of each 21 subject are represented in thin lines. Some subjects overlap each other in some places.

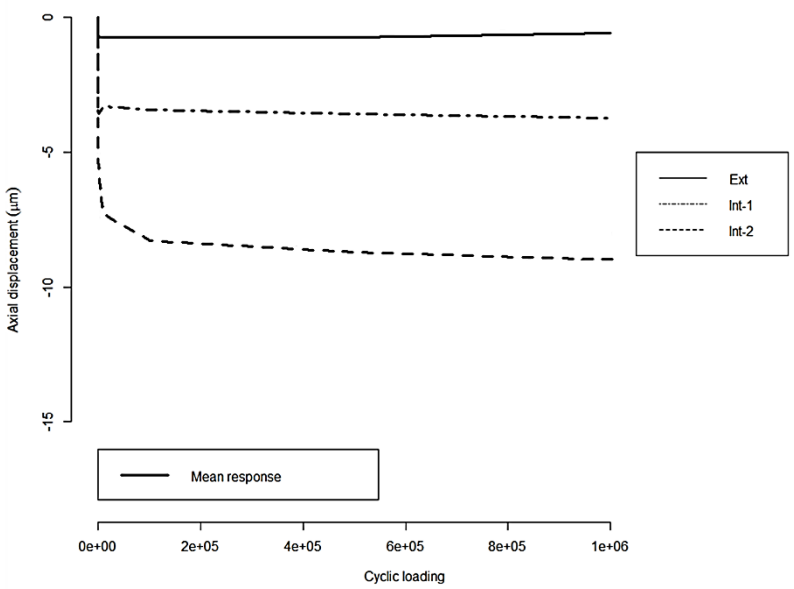

Fig. 12-2. The mean response curve of each group are represented in thick lines.

As the length of the implant-abutment assembly were measured at the time of exponential cycles (10^n), the number of cycles were converted to common logarithmic scale for convenience in the calculation. The conversion formula was as follows:

$$t' = log_{10}(t + 1) \qquad [1]$$

where t is the time (number of cycles). In the formula, t was converted to $t + 1$ because $log_{10}(0)$ in initial measurement at cycle 0 have a negative value of infinity (-∞). The change from "t" to " $t + 1$" have a negligible effect on the analysis by the linear mixed model.

After the conversion to the curve in logarithmic scale, the patterns were almost linear with slight bending (Fig. 13-1 and -2).

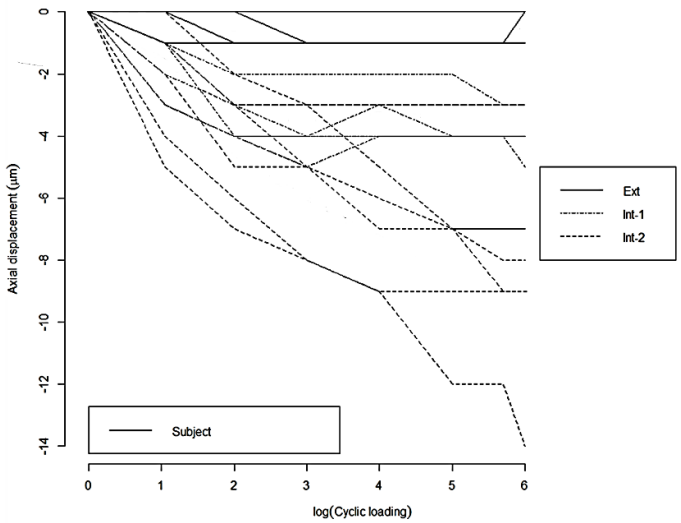

Fig. 13-1. The individual patterns of each specimen are represented in thin lines. Some subjects overlap each other in some places.

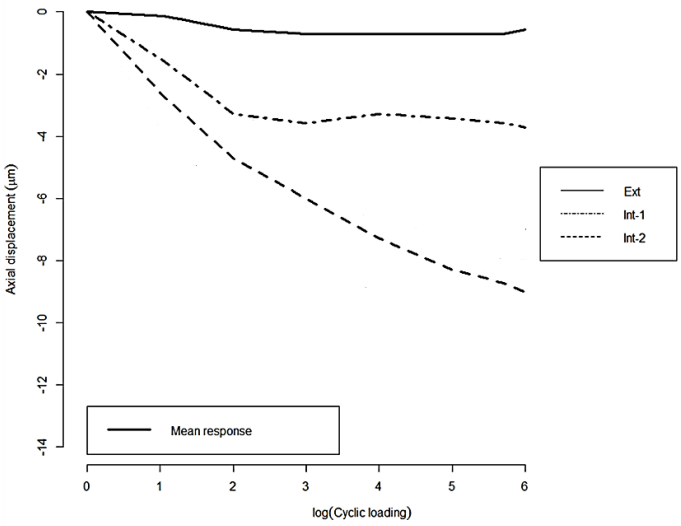

Fig. 13-2. The mean response curves of each group in logarithmic scale are represented in thick lines.

In the linear mixed model, the following statistical formula was drawn.

$$Y_i = \beta_{i0} + (t - x)_+ \beta_{i1} + (x - t)_+ \beta_{i2} \qquad [2]$$

The formula above can be divided as follows.

$$Y_i = \beta_{i0} + t\beta_{i1} - \beta_{i1}x \qquad \text{if} \quad x \leq t \qquad [3\text{-}1]$$

$$Y_i = \beta_{i0} - t\beta_{i2} + \beta_{i2}x \qquad \text{if} \quad x > t \qquad [3\text{-}2]$$

where the β_{i0} is the intercept at breakpoint, $-\beta_{i1}$ is the slope before the breakpoint, β_{i2} is the slope after the breakpoint, t is the time (number of cycles), i is the group (1: Ext group, 2: Int-1 group, 3: Int-2 group), and *1*, *2* are the cycles (1: cycle before the breakpoint, 2: cycle after the breakpoint).

According to the formula, the patterns in logarithmic scale were fitted as followings (Fig. 14-1 and -2).

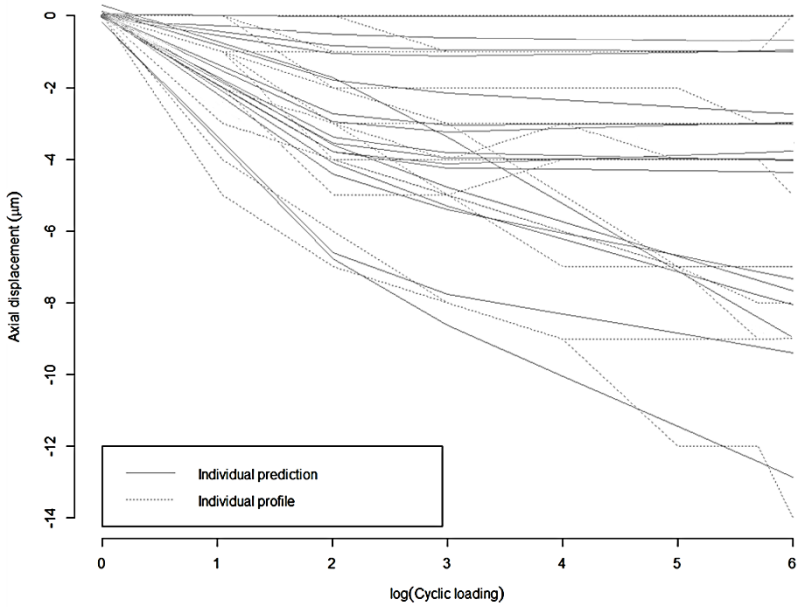

Fig. 14-1. The individual profiles and predictions of each 21 subject are represented in dotted lines and solid lines, respectively, in logarithmic scale.

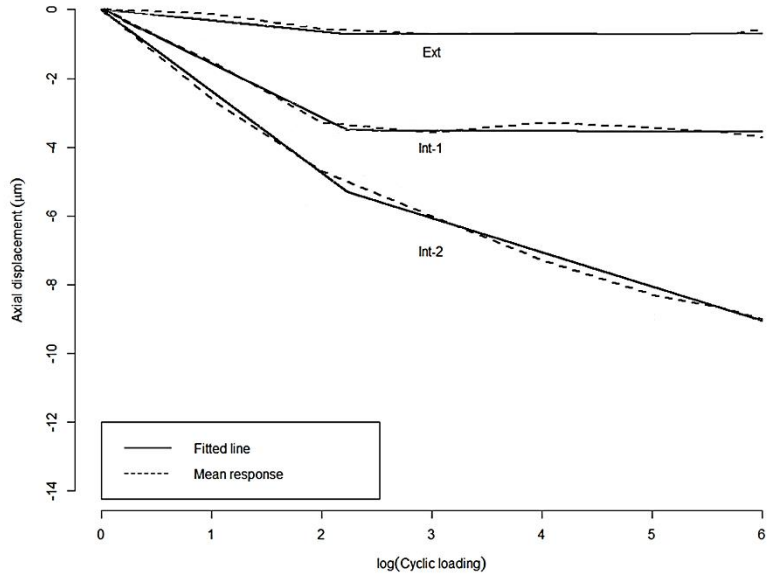

Fig. 14-2. The fitted models of patterns in logarithmic scale. The patterns were fitted well compared with the mean response curve.

The patterns in logarithmic scale of each group revealed a breakpoint at 2.24, which was original value of at 171 cycles.

Table VIII. The patterns of axial displacement with a breakpoint at 2.24 in logarithmic scale

coefficient	estimate	SE	t value	*P* -value
β_{10}	-0.72	0.5184	-1.391	0.1796
β_{20}	-3.51	0.5184	-6.771	<0.0001
β_{30}	-5.31	0.5184	-10.243	<0.0001
β_{11}	-0.32	0.2298	1.407	0.1748
β_{12}	0.00	0.1284	0.024	0.9811
β_{21}	-1.57	0.2298	6.838	<0.0001
β_{22}	-0.01	0.1284	-0.101	0.92056
β_{31}	-2.38	0.2298	10.342	<0.0001
β_{32}	-1.00	0.1284	-7.751	<0.0001

SE: standard error. In βab, "β" denotes a regression coefficient, subscript "a" refer to the group (1: Ext group, 2: Int-1 group, 3: Int-2 group), and subscript "b" refer to the cycle (0: cycle at 2.24, 1: cycle ≤ 2.24, 2: cycle > 2.24 in logarithmic scale).

In the Table VIII, the value of β_{10} with -0.72 means that the amount of axial displacement was 0.72 μm at 171 cycles. In the Ext group (β_{11}, β_{12}), the declining pattern was not found before and after the breakpoint ($P > 0.05$), which means that axial displacement did not occur.

In the Int-1 group, the value of β_{20} with -3.51 means that the amount of axial displacement was 3.51 μm at 171 cycles. According to the value of β_{21} and β_{22}, significant declining pattern was found in the before of the breakpoint with slope

of -1.57. However, no significant declining pattern was found after the breakpoint with slope of -0.01 ($P > 0.05$).

In the Int-2 group, the value of β_{30} with -5.31 means that the amount of axial displacement was 5.31 μm at 171 cycles. According to the value of β_{31} and β_{32}, significant declining pattern was found before the breakpoint with slope of -2.38. After the breakpoint, the declining pattern was also found with slope of -1.00 ($P < 0.05$). That is, the Int-2 group showed continuous axial displacement before and after the breakpoint.

The patterns in logarithmic scale were converted to in original value as followings (Fig. 15-1 and -2). The plateau of the Ext and Int-1 group can be easily detected at early phase (171 cycles). Both group showed no more axial displacement after the breakpoint ($P = 0.98$ and 0.92, respectively). In the Int-2 group, the exact point of plateau was hardly figured out. However, at a glance, the rate of axial displacement slowed after about 100,000 cycles, where the amount of axial displacement is 8.1 μm. After the 100,000 cycles, the changes in the amount of axial displacement could be interpreted as more stable than before the 100,000 cycles (Table IX).

Table IX shows the fitted data of axial displacement. The values of each cycle are comparable with raw data shown in Table VII.

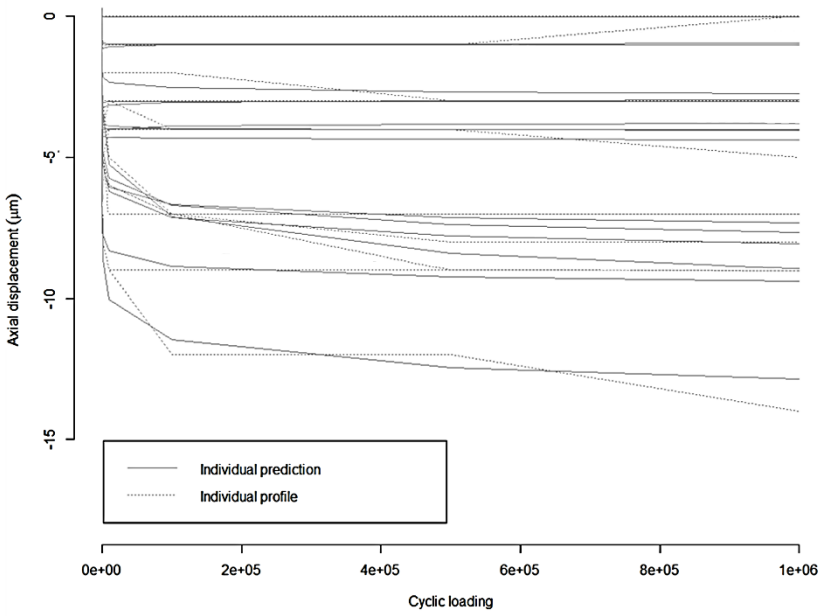

Fig. 15-1. The individual profiles and predictions of each 21 subject were converted to the graphs in original value, which were represented in dotted lines and solid lines, respectively.

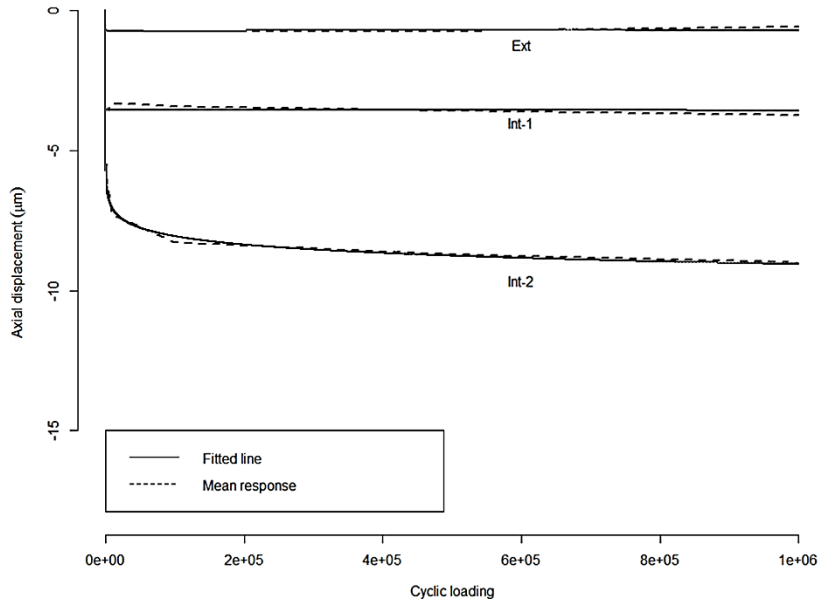

Fig. 15-2. The fitted models in original values. The patterns were fitted well compared with the mean response curve.

Table IX. The fitted data of axial displacement of abutment at each cycle by pattern analysis with linear mixed model (μm)

Cycles	Group		
	Ext	Int-1	Int-2
0	0.0	0.0	0.0
10	-0.3	-1.6	-2.5
100	-0.6	-3.1	-4.8
1,000	-0.7	-3.5	-6.1
10,000	-0.7	-3.5	-7.1
100,000	-0.7	-3.5	-8.1
500,000	-0.7	-3.6	-8.8
1,000,000	-0.7	-3.6	-9.1

Ext: External type implant; Int-1: Internal type implant with one-piece abutment; Int-2: Internal type implant with two-piece abutment.

5. Microscopic computed tomography

The microscopic computed tomography (micro-CT) was taken for one sample per group to identify the internal structures. The micro-CT images were examined with relevant software program (DataViewer®, version 1.5, SKYSCAN, Belgium). The sagittal images of Ext group were identical at an interval of 60 degree, and the two representative images were shown repeatedly at an interval of 30 degree (Fig.16). The sagittal images of Int-1 and Int-2 group were identical at an interval of 90 degree for each group, and the two representative images were shown repeatedly at an interval of 45 degree (Fig. 18 and 20). The axial images of specimens were all examined, and the representative images were shown in Fig 17, 19, and 21.

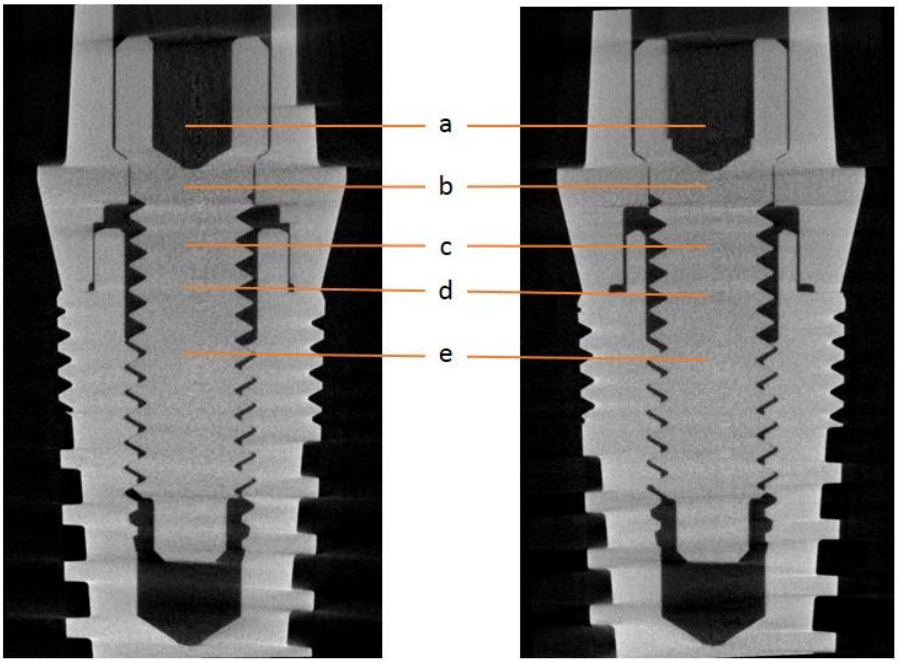

Fig. 16. The micro-CT images of Ext group. The representative two images at an interval of 30 degree. The images at **a**, **b**, **c**, **d**, and **e** are presented in Fig. 17.

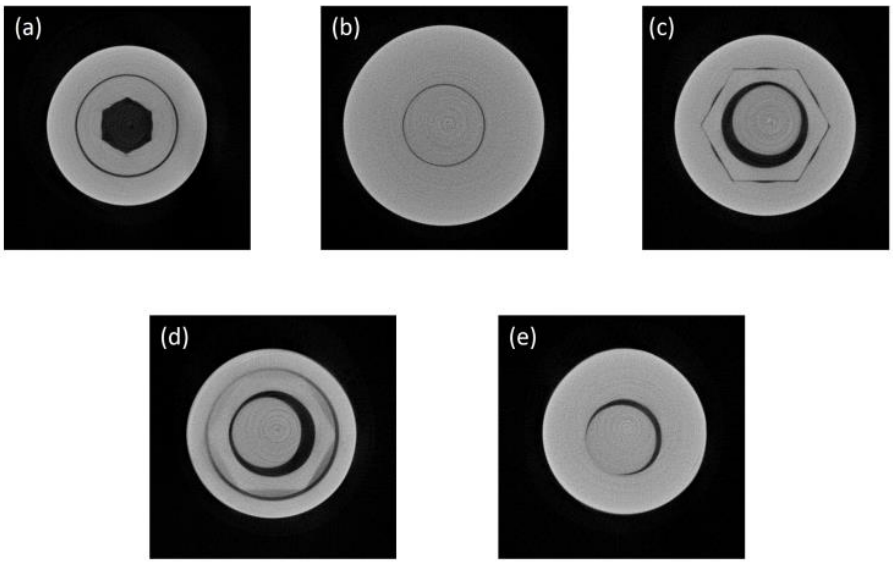

Fig. 17. The axial slice images of Ext group at each location marked in Fig. 16.

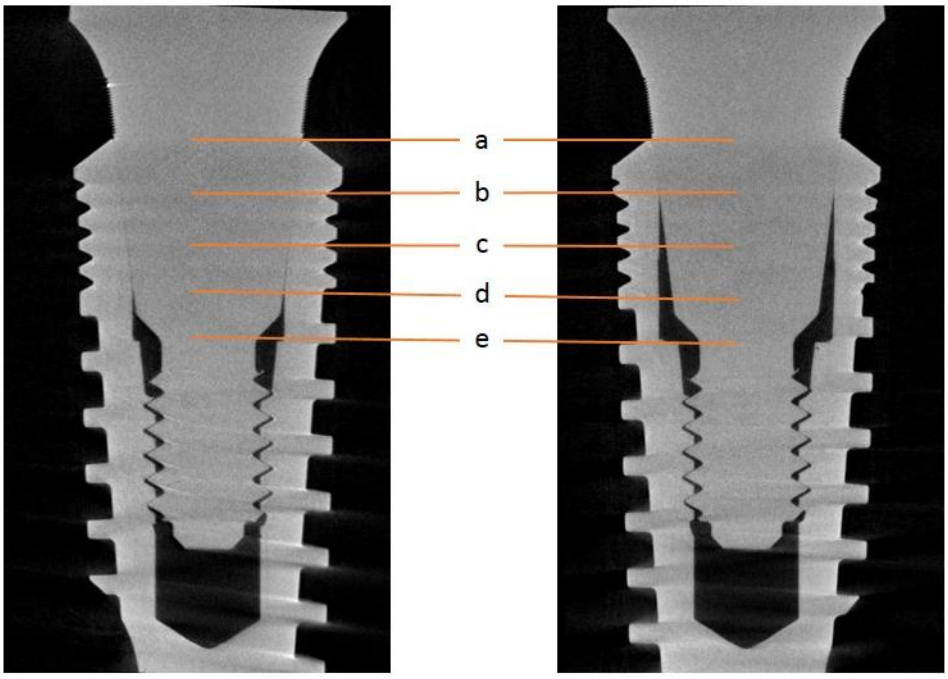

Fig. 18. The micro-CT images of Int-1 group. The representative two images at an interval of 45 degree. The images at **a**, **b**, **c**, **d**, and **e** are presented in Fig. 19.

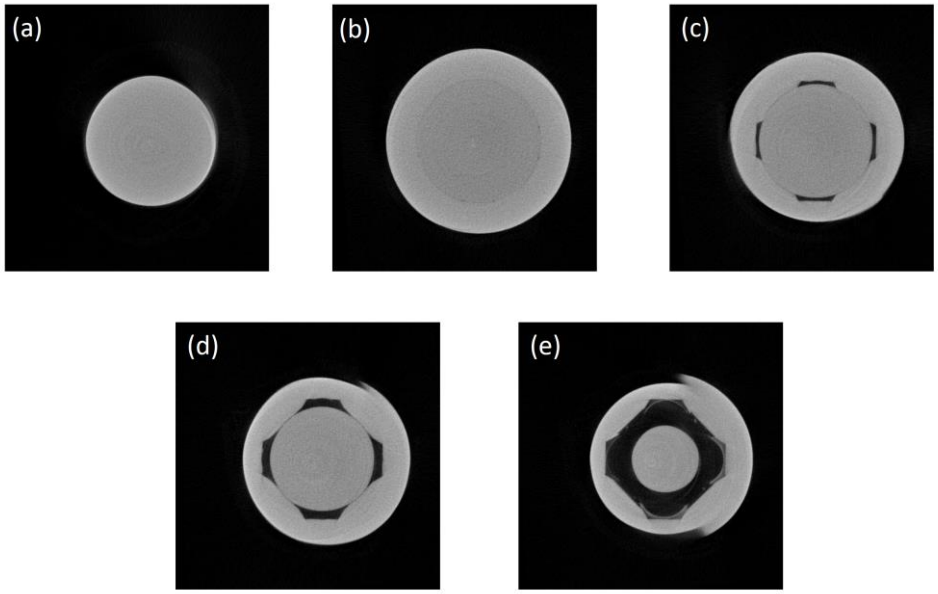

Fig. 19. The axial slice images of Int-1 group at each location marked in Fig. 18.

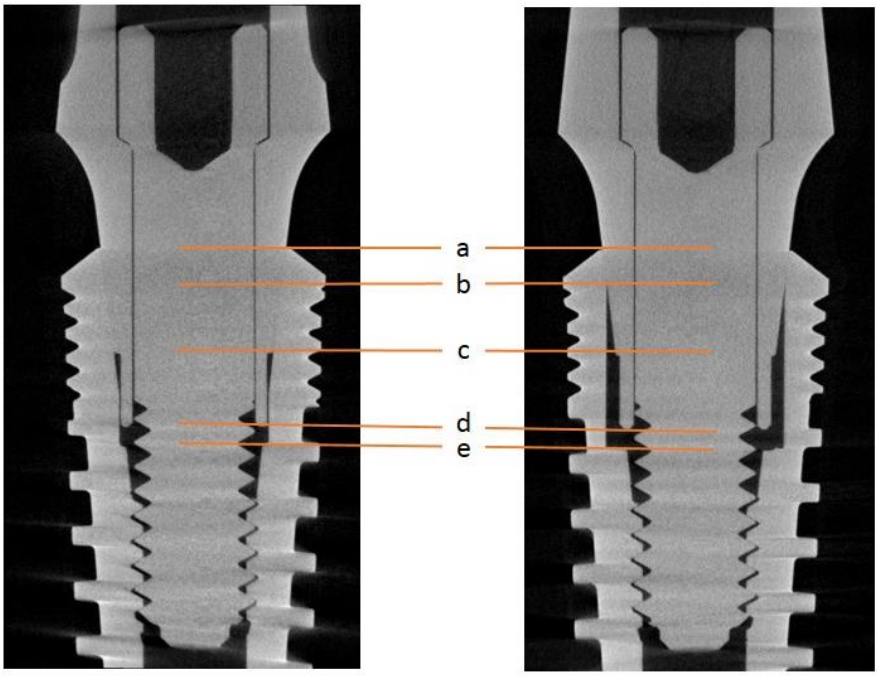

Fig. 20. The micro-CT images of Int-2 group. The representative two images at an interval of 45 degree. The images at **a**, **b**, **c**, **d**, and **e** are presented in Fig. 21.

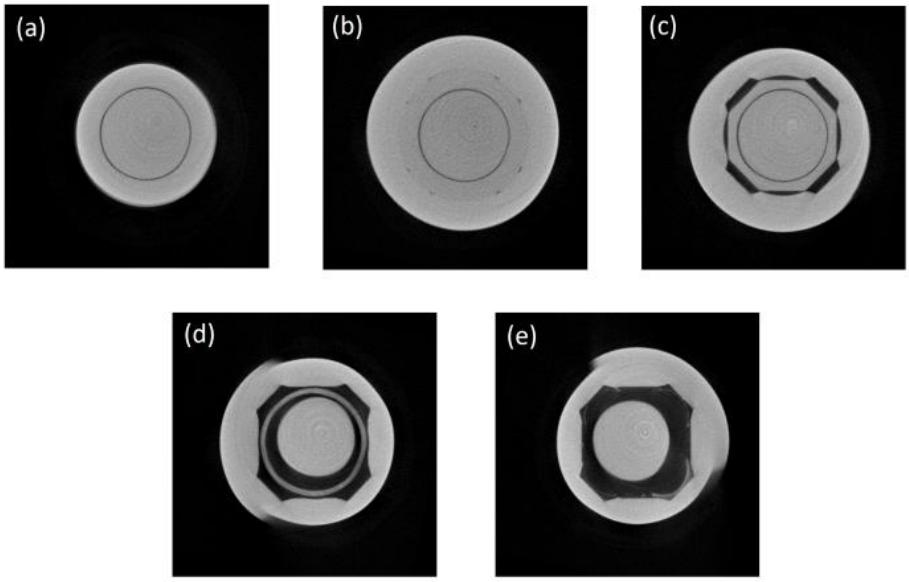

Fig. 21. The axial slice images of Int-2 group at each location marked in Fig. 20.

The maximum length of contact in tapered connection of Int-2 group is relatively shorter than that of Int-1 group, as described in Table III. Because the anti-rotational structure with octagon was integrated to tapered part of abutment, the length of contact have been, of course, diminished.

6. Scanning electronic microscopic evaluation

The SEM images of Ext group are shown in Fig 22. The round index around external hex remained intact as machined by manufacturer. However, the surface of fretting wear[40, 41] was noticed at the surface of implant and abutment. The area of fretting wear was broader in the implant than in the abutment.

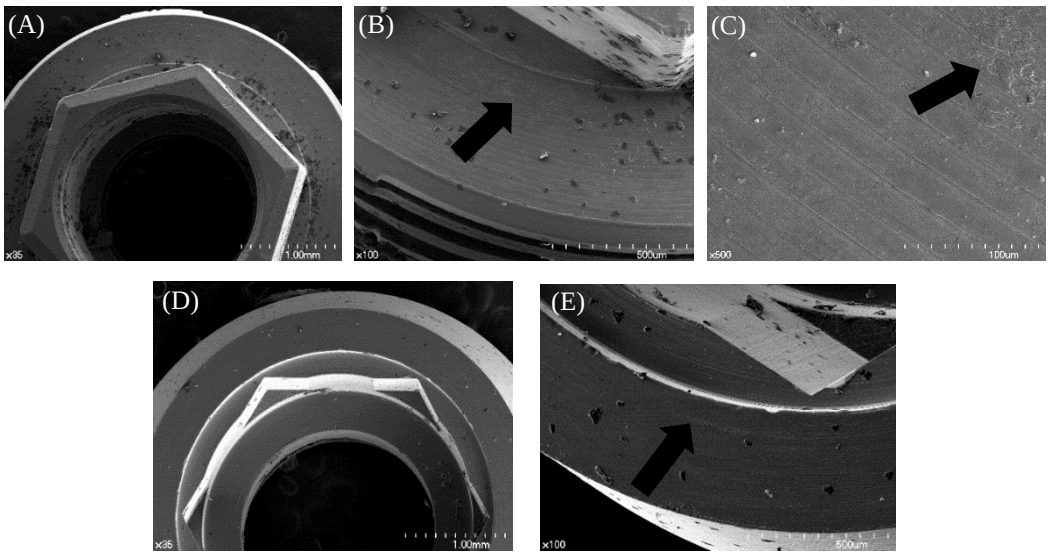

Fig. 22. The SEM images of Ext group. The black arrow designates a fretting wear. Images of the platform of implant (**A**: ×35, **B**: ×100, **C**: ×500 magnification) and images of abutment (**D**: ×35, **E**: ×100 magnification) are shown.

The SEM images of Int-1 group are shown in Fig 23. The adhesive wear[42] was noticed as marked in black arrow. More wear/plastic deformation was found at internal surface of implant than that of abutment. The microroughness in intact surface was deformed by sliding motion during abutment connection and cyclic loading.

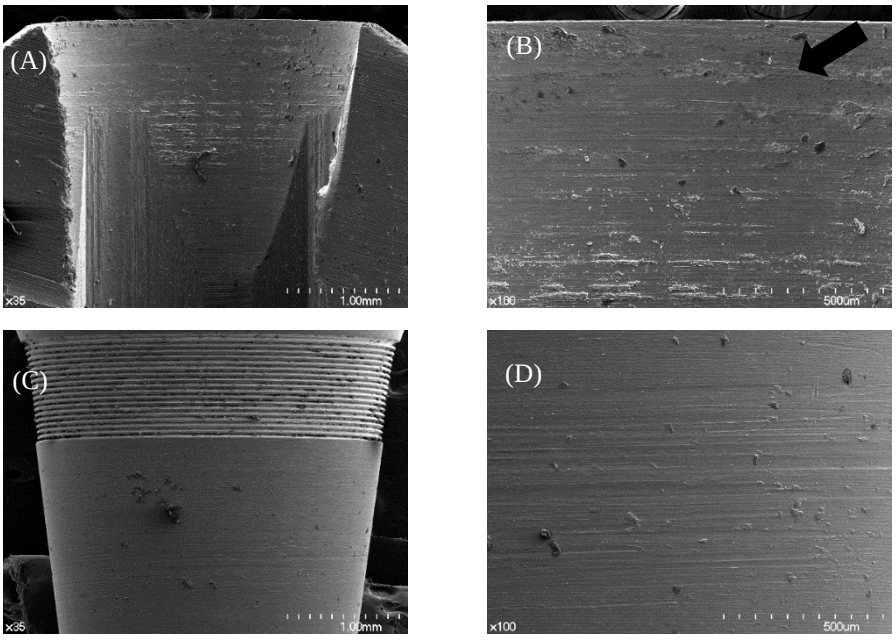

Fig. 23. The SEM images of Int-1 group. Images of the internal surface of tapered connection of implant (**A**: ×35, **B**: ×100 magnification) and images of abutment (**C**: ×35, **D**: ×100 magnification) are shown. The black arrow indicates the adhesive wear, which was a result from that the abutment was connected helically following the screw thread.

The SEM images of Int-2 group are shown in Fig 24. Both the adhesive wear area and intact machined surface were noticed as marked in black arrow and black arrow head, respectively.

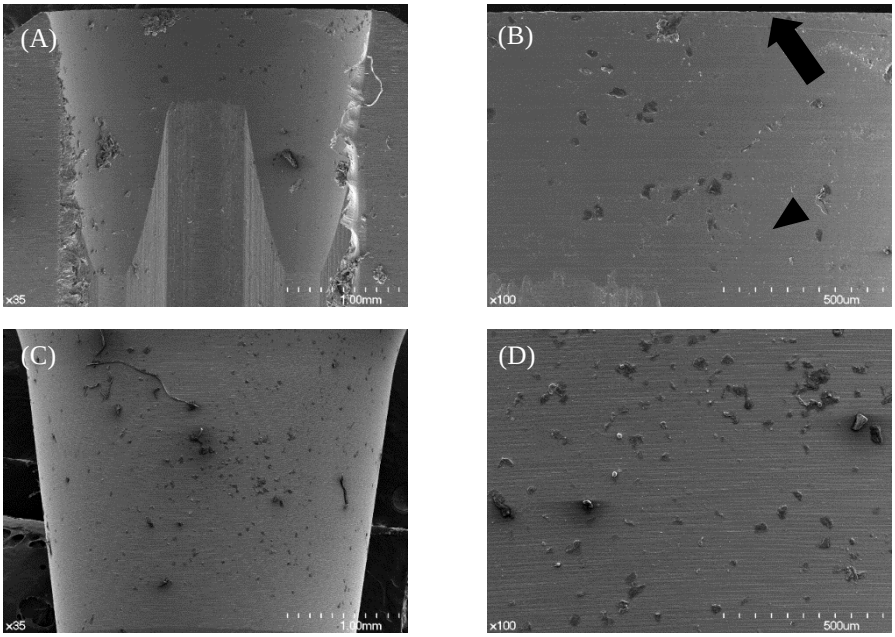

Fig. 24. The SEM images of Int-2 group. Images of the internal surface of tapered connection of implant (**A**: ×35, **B**: ×100 magnification) and images of abutment (**C**: ×35, **D**: ×100 magnification) are shown. The adhesive wear, marked in black arrow, are limited to the most coronal part of implant. The machined surface, marked in arrow head, remained intact.

The wear/plastic deformation in Int-2 group were found less than in Int-1 group. Only the most coronal portion showed adhesive wear, and the other area showed almost intact machined surface. The significant difference between Int-1 and Int-2 group in the amount of wear/plastic deformation might be the result of connection system, that is, the tapered abutment was integrated to the screw or not.

IV. DISCUSSION

The present study was conducted to assess the effect of cyclic loading on abutment with internally tapered connected implant. The analysis about the patterns of the axial displacement of implant-abutment assembly after cyclic loading in internal tapered connection system was performed, and the authors tried to figure out the plateau in the amount of axial displacement. The internal structures and surface characteristics of implant-abutment assemblies were analyzed by micro-CT and SEM, respectively.

The authors adopted the collet and nut system in measuring the axial displacement of abutment into the implant after repeated tightening torque. This system enabled the authors to mount and disassemble the abutment-implant assemblies from the implant holder with convenience. In virtue of simplicity of mounting, the length of implant-abutment assemblies were measured whenever it was necessary. The length of the implant-abutment assembly were measured easily at exponential pattern of cyclic loadings (10^n).

In a recent study about removal torque of abutment after repeated insertion/removal procedures in implants with internal tapered connections,[43] a linear mixed model was used only to compare the removal torque values among the groups and the cycles. The changes in removal torque value of abutment with the course of time was not provided in that study, but was only described in the table

and box-plot graph.

On the other hand, in the present study, the linear mixed model (package lme4) with R Statistics was utilized to figure out the patterns of axial displacement with time (cyclic loading). The model gave the authors an effective tool in finding out the plateau in each group. As the result, the rate of axial displacement with a course of cyclic loading were found.

The PTVs were measured before and after the cyclic loading. Although the PTV in Int-2 group decreased with statistically significance, the value of -6.7 could be regarded as stable. Since the periotest value up to -3 to -2 has been generally accepted as clinically stable status of the implant-abutment connection,[44] the stability of implant-abutment connection could be favorable. In the Ext and Int-1 group showed no changes in the PTV with range from -7.7 to -7.4.

The RTVs were also measured before and after the cyclic loading. The RTVs before the cyclic loading were almost same with tightening torque in Ext and Int-2 group, and were higher in Int-1 group which have a tapered interference fit in implant-abutment connection. In general, the static friction coefficient shows higher value than kinetic friction coefficient. In this regard, the loosening torque would be higher than tightening torque. After the cyclic loading, the RTVs were changed significantly. Int-2 group showed removal torque of 15.6 Ncm (52 % compared to tightening torque). The authors reasoned that the decrease of RTV in Int-2 group were primarily from axial displacement of abutment into implant. Due to the axial

displacement of abutment, the preload of the screw would be diminished, so that the removal torque have decreased.

Most of the tightening torque was converted to frictional force in tapered connection, and only about 10% or less was participated in the screw preload.[22] Therefore, it can be speculated that the implant-abutment connection remained stable even though the screw loosening occurred in Int-2 group.

However, since this study simulated only vertical forces to implant-abutment assembly, the clinical relevance could be diminished. It must be considered in clinical situation that the lateral force to the abutment might jeopardize the stability of the connection.

In the evaluation by the micro-CT images, the abutment of Int-2 group have a cylinder-like structure, since the tapered abutment and the screw are separated. Therefore, the two-piece abutment might not able to withstand the vertical and normal forces from cyclic loading than one-piece abutment do. In this regard, the plastic deformation or wear might occur easily, which may result in axial displacement. This would be the main cause of the difference between Int-1 and Int-2 abutment.

In the SEM images of platform of Ext group, the fretting wear/plastic deformation was noticed. It has been known that vibration and micromovement induce the fretting wear.[40, 41] Fretting wear occurs when repeated loading cause cyclic stresses that induce surfaces or subsurface breakup, resulting in the loss of

material. A portion of the amount of axial displacement of Ext group could be explained by the fretting wear. The elastic modulus of implant composed of Ti grade 4 is 105 GPa and that of abutment is 113.8 GPa (Ti grade 5, Ti-6Al-4V). As the result, more wear of the surface of implant was noticed than that of abutment in the butt-joint interface (Fig. 22).

In the same way, it can be explained that the wear of abutment in Int-1 and Int-2 group showed less amount than that of implant. The internal aspect of tapered connection showed significant adhesive wear, especially in Int-1 group. The adhesive wear, also known as galling, is a result of the high contact stresses.[42] The high local stresses deform the material plastically at the contact points. As the force causing the sliding motion increases, the shear stress increases. This results in transfer of material into the region between the solids. In the tapered integrated screwed-in (TIS) abutment, only 10% of the clamping force are converted to screw preload.[22] Most of the clamping force are exerted to overcome the frictional force. Therefore, it can be deduced that the frictional force have induced the adhesive wear. The internal aspect of Int-2 group show less adhesive wear than Int-1 group. As a result, it could be deduced that the less clamping force were converted to frictional force than in Int-1 group.

The amount of axial displacement after tightening torque in this study was comparable with the results of earlier study which reported 4.2 μm in external group and 48.6 μm in 11° tapered internal hexagonal with two-piece abutment.[28]

The amount of axial displacement after cyclic loading in this study was also comparable with an early study.[31] The external type implant with a flat platform interface showed least amount of axial displacement (2.5 μm for external implant group), and more axial displacement was found at internal tapered implant (8.1 μm for internal implant group) after 1 million cycles of 250 N loading for abutment-replica system with 30 Ncm tightening.

In the raw data of measurement, the Ext group showed 0.6 μm of axial displacement at 1,000,000 cycles. In the pattern analysis, no axial displacement was found in Ext group. As the additional axial displacement was not noticed after 1,000 cycles in the Ext group with a total amount of less than 1 μm. The axial displacement of external butt-joint implant can be neglected in clinical situations. Therefore, clinicians do not need to wait for settling occur. And, in the clinical case of vertical stability is essential, the external butt-joint implant would be more appropriate.

Internal tapered implant showed more axial displacement than external type implant. In the internal tapered connection design, a certain amount of axial displacement of abutment into implant according to the applied cyclic loading were found until 171 cycles, and no more axial displacement after the cycles, at which the plateau was found with a value of 3.5 μm. It is in accordance with explanation by Bozkaya and Muftu that axial location of tapered interference fit would converge on the certain extent.[20-22]

Int-2 group showed more axial displacement than Int-1 group. Between Int-1 and Int-2 groups, the values of axial displacement became statistically different after 10,000 cycles. However, in Int-2 group, continuous axial displacement in implant-abutment assemblies were found after breakpoint of 171 cycles without any plateau.

The slope of -1.00 after breakpoint means that the amount of axial displacement increase in 1 μm as the cycles of loading increase in exponential (10^n). In this regard, in 10^7 cycles, the total amount of axial displacement could be speculated 10 μm, and 11 μm in 10^8 cycles.

To estimate the time needed for enough settling, corresponded cycles to chronological time period is required. However, the time period equivalent to one year varies with the literatures that 50,000 cycles,[45, 46] 250,000 cycles,[47] 800,000 cycles,[34] or 1,000,000 cycles[48, 49] corresponds to one year. The authors adopted the result that one year corresponds to 1,000,000 cycles.

According to the assumption that one year corresponds one million cycles, the breakpoint of 171 cycles in Int-1 group corresponds to 1.5 hours. Therefore, the axial displacement of one-piece abutment (Int-1) could be achieved within one day.

As described in Fig. 15 and Table IX about Int-2 group, the increment of axial displacement after 100,000 cycles could be neglected in clinical aspect due to the slope with -1.00 in the pattern analysis. Therefore, the time near to plateau could be speculated around 100,000 cycles. Considering that the 100,000 cycles correspond to about one month,[48, 49] most of the axial displacement of internal two-piece

abutment in clinical situation might occur within one month after the delivery of abutment.

Two-piece abutment system including CAD-CAM abutment was recently popularized for biocompatible emergence profile and for providing consistent direction of abutment in laboratory and clinical procedure. However, the axial displacement according to the tightening torque can be about 48 μm according to the present study. It is beyond the threshold of tactile sense in natural teeth and implant.[50, 51] Therefore, the abutment is recommended to be tightened enough according to the manufacturer's instruction.

The cyclic loading after repeated tightening have induced 9 μm settling in this study. It is within the threshold of natural teeth and implant, but is comparable with the thickness of occlusion test foil (8 μm, Shimstock, Hanel, Contene/Whaledent, Germany). A patient with high tactile sensitivity might be able to discriminate the amount of 9 μm after chewing behavior.[50] Therefore, the axial displacement of 9 μm might discomfort the patient in tactile sensitivity.

In addition, it was already stated that screw loosening was more likely to occur during the first month of function.[52] Therefore, in the two-piece abutment system, the time period of at least one month in oral environment is recommended before the retightening of abutment and the impression for definitive prosthesis.

This study was conducted with a specific implant system with 7° taper and internal octagonal structure, so the results of the present study may not provide

generalized conclusion for other systems which include 8° tapered or 11° tapered, internal hexagonal or dodecagonal, or without any anti-rotational structure. Therefore, the patterns of axial displacement cannot be applied generally to all implant systems. Additional experiments is recommended to identify the patterns of the other implant systems.

V. CONCLUSIONS

Within the limitations of this study, the following conclusions can be drawn:

1. The axial displacements according to the tightening torque occurred in all groups.
2. The surface wear of the implant-abutment connection after cyclic loading were noticed in all groups.
3. The periotest values remained stable, but the removal torque value decreased after cyclic loading in all groups.
4. In the analysis by linear mixed model, Ext and Int-1 group showed the plateau of axial displacement at early phase of cyclic loading. The exact point of plateau was hardly figured out in Int-2 group, but the rate of axial displacement slowed after 100,000 cycles.

This study demonstrated the patterns of axial displacement in internal implant system and the decrease in removal torque value. In the clinical aspect, it is recommended that the screw be retightened after at least one month to minimize the screw loosening and clinical prosthetic errors.

REFERENCES

1. Albrektsson T. A multicenter report on osseointegrated oral implants. J Prosthet Dent 1988;60(1):75-84.
2. Jemt T. Fixed implant-supported prostheses in the edentulous maxilla. A five-year follow-up report. Clin Oral Implants Res 1994;5(3):142-7.
3. Buser D, Mericske-Stern R, Bernard JP, Behneke A, Behneke N, Hirt HP, et al. Long-term evaluation of non-submerged ITI implants. Part 1: 8-year life table analysis of a prospective multi-center study with 2359 implants. Clin Oral Implants Res 1997;8(3):161-72.
4. Jemt T. Failures and complications in 391 consecutively inserted fixed prostheses supported by Branemark implants in edentulous jaws: a study of treatment from the time of prosthesis placement to the first annual checkup. Int J Oral Maxillofac Implants 1991;6(3):270-6.
5. Binon PP. The effect of implant/abutment hexagonal misfit on screw joint stability. Int J Prosthodont 1996;9(2):149-60.
6. Goodacre CJ, Bernal G, Rungcharassaeng K, Kan JY. Clinical complications with implants and implant prostheses. J Prosthet Dent 2003;90(2):121-32.
7. Jemt T, Pettersson P. A 3-year follow-up study on single implant treatment. J Dent 1993;21(4):203-8.
8. Sutter F, Weber HP, Sorensen J, Belser U. The New Restorative Concept of the ITI Dental Implant System: Design and Engineering. Int J Periodontics Restorative Dent 1993;13(5):408-31.
9. Norton MR. Assessment of cold welding properties of the internal conical

interface of two commercially available implant systems. J Prosthet Dent 1999;81(2):159-66.

10. Merz BR, Hunenbart S, Belser UC. Mechanics of the implant-abutment connection: an 8-degree taper compared to a butt joint connection. Int J Oral Maxillofac Implants 2000;15(4):519-26.
11. Khraisat A, Stegaroiu R, Nomura S, Miyakawa O. Fatigue resistance of two implant/abutment joint designs. J Prosthet Dent 2002;88(6):604-10.
12. Kitagawa T, Tanimoto Y, Odaki M, Nemoto K, Aida M. Influence of implant/abutment joint designs on abutment screw loosening in a dental implant system. J Biomed Mater Res B Appl Biomater 2005;75(2):457-63.
13. Norton MR. An in vitro evaluation of the strength of an internal conical interface compared to a butt joint interface in implant design. Clin Oral Implants Res 1997;8(4):290-8.
14. Arvidson K, Bystedt H, Frykholm A, von Konow L, Lothigius E. Five-year prospective follow-up report of the Astra Tech Dental Implant System in the treatment of edentulous mandibles. Clin Oral Implants Res 1998;9(4):225-34.
15. Schwarz MS. Mechanical complications of dental implants. Clin Oral Implants Res 2000;11 Suppl 1(s1):156-8.
16. Tesmer M, Wallet S, Koutouzis T, Lundgren T. Bacterial colonization of the dental implant fixture-abutment interface: an in vitro study. J Periodontol 2009;80(12):1991-7.
17. Aloise JP, Curcio R, Laporta MZ, Rossi L, da Silva AM, Rapoport A. Microbial leakage through the implant-abutment interface of Morse taper implants in vitro. Clin Oral Implants Res 2010;21(3):328-35.
18. Harder S, Dimaczek B, Acil Y, Terheyden H, Freitag-Wolf S, Kern M.

Molecular leakage at implant-abutment connection--in vitro investigation of tightness of internal conical implant-abutment connections against endotoxin penetration. Clin Oral Investig 2010;14(4):427-32.

19. do Nascimento C, Miani PK, Pedrazzi V, Goncalves RB, Ribeiro RF, Faria ACL, et al. Leakage of Saliva Through the Implant-Abutment Interface: In Vitro Evaluation of Three Different Implant Connections Under Unloaded and Loaded Conditions. Int J Oral Maxillofac Implants 2012;27(3):551-60.
20. Bozkaya D, Muftu S. Mechanics of the tapered interference fit in dental implants. J Biomech 2003;36(11):1649-58.
21. Bozkaya D, Muftu S. Efficiency considerations for the purely tapered interference fit (TIF) abutments used in dental implants. J Biomech Eng 2004;126:393.
22. Bozkaya D, Muftu S. Mechanics of the taper integrated screwed-in (TIS) abutments used in dental implants. J Biomech 2005;38(1):87-97.
23. Dailey B, Jordan L, Blind O, Tavernier B. Axial Displacement of Abutments into Implants and Implant Replicas, with the Tapered Cone-Screw Internal Connection, as a Function of Tightening Torque. Int J Oral Maxillofac Implants 2009;24(2):251-56.
24. Gratton DG, Aquilino SA, Stanford CM. Micromotion and dynamic fatigue properties of the dental implant-abutment interface. J Prosthet Dent 2001;85(1):47-52.
25. Cantwell A, Hobkirk JA. Preload loss in gold prosthesis-retaining screws as a function of time. Int J Oral Maxillofac Implants 2004;19(1):124-32.
26. Bakaeen LG, Winkler S, Neff PA. The effect of implant diameter, restoration design, and occlusal table variations on screw loosening of posterior single-

tooth implant restorations. J Oral Implantol 2001;27(2):63-72.

27. Siamos G, Winkler S, Boberick KG. Relationship between implant preload and screw loosening on implant-supported prostheses. J Oral Implantol 2002;28(2):67-73.
28. Kim KS, Lim YJ, Kim MJ, Kwon HB, Yang JH, Lee JB, et al. Variation in the total lengths of abutment/implant assemblies generated with a function of applied tightening torque in external and internal implant-abutment connection. Clin Oral Implants Res 2011;22(8):834-9.
29. Byrne D, Jacobs S, O'Connell B, Houston F, Claffey N. Preloads generated with repeated tightening in three types of screws used in dental implant assemblies. J Prosthodont 2006;15(3):164-71.
30. Shigley J, Mischke C, Brown T. Standard Handbook of Machine Design. 3rd ed: McGraw-Hill Professional, 2004:22.28.
31. Lee JH, Kim DG, Park CJ, Cho LR. Axial displacements in external and internal implant-abutment connection. Clin Oral Implants Res 2012:1-7.
32. Kim SK, Koak JY, Heo SJ, Taylor TD, Ryoo S, Lee SY. Screw loosening with interchangeable abutments in internally connected implants after cyclic loading. Int J Oral Maxillofac Implants 2012;27(1):42-7.
33. Richter EJ. In vivo vertical forces on implants. Int J Oral Maxillofac Implants 1995;10(1):99-108.
34. Rosentritt M, Behr M, Gebhard R, Handel G. Influence of stress simulation parameters on the fracture strength of all-ceramic fixed-partial dentures. Dent Mater 2006;22(2):176-82.
35. R Development Core Team. R: A language and environment for statistical computing. R Foundation for Statistical Computing. Vienna, Austria. 2013.

http://www.R-project.org.

36. Bates D, Maechler M, Bolker B. lme4: Linear mixed-effects models using S4 classes. R package version 0.999999-2. 2013. http://CRAN.R-project.org/package=lme4.
37. Cnaan A, Laird N, Slasor P. Tutorial in biostatistics: using the general linear mixed model to analyse unbalanced repeated measures and longitudinal data. Stat Med 1997;16:2349-80.
38. Schall R. Estimation in Generalized Linear-Models with Random Effects. Biometrika 1991;78(4):719-27.
39. Winter B. Linear models and linear mixed effects models in R with linguistic applications. arXiv:1308.5499. 2013: [http://arxiv.org/pdf/1308.5499.pdf].
40. Brodbeck U. The ZiReal Post: A new ceramic implant abutment. J Esthet Restor Dent 2003;15(1):10-23; discussion 24.
41. Klotz MW, Taylor TD, Goldberg AJ. Wear at the titanium-zirconia implant-abutment interface: a pilot study. Int J Oral Maxillofac Implants 2011;26(5):970-5.
42. Schaffer JP, Saxena A, Antolovich SD, Sanders T, Warner SB. The science and design of engineering materials. 2nd ed. Singapore; WCB/McGraw-Hill; 1999. p. 655-58.
43. Ricciardi Coppede A, de Mattos Mda G, Rodrigues RC, Ribeiro RF. Effect of repeated torque/mechanical loading cycles on two different abutment types in implants with internal tapered connections: an in vitro study. Clin Oral Implants Res 2009;20(6):624-32.
44. Cehreli MC, Akca K, Iplikcioglu H, Sahin S. Dynamic fatigue resistance of implant-abutment junction in an internally notched morse-taper oral implant:

influence of abutment design. Clin Oral Implants Res 2004;15(4):459-65.

45. Sakaguchi RL, Douglas WH, DeLong R, Pintado MR. The wear of a posterior composite in an artificial mouth: a clinical correlation. Dent Mater 1986;2(6):235-40.
46. Hakimeh S, Vaidyanathan J, Houpt ML, Vaidyanathan TK, Von Hagen S. Microleakage of compomer class V restorations: effect of load cycling, thermal cycling, and cavity shape differences. J Prosthet Dent 2000;83(2):194-203.
47. Outhwaite WC, Twiggs SW, Fairhurst CW, King GE. Slots vs pins: a comparison of retention under simulated chewing stresses. J Dent Res 1982;61(2):400-2.
48. Winkler S, Ring K, Ring JD, Boberick KG. Implant screw mechanics and the settling effect: overview. J Oral Implantol 2003;29(5):242-5.
49. Wiskott HW, Nicholls JI, Belser UC. Stress fatigue: basic principles and prosthodontic implications. Int J Prosthodont 1995;8(2):105-16.
50. Lundqvist S, Haraldson T. Occlusal perception of thickness in patients with bridges on osseointegrated oral implants. Scand J Dent Res 1984;92(1):88-92.
51. Jacobs R, van Steenberghe D. Role of periodontal ligament receptors in the tactile function of teeth: a review. J Periodontal Res 1994;29(3):153-67.
52. Breeding LC, Dixon DL, Nelson EW, Tietge JD. Torque required to loosen single-tooth implant abutment screws before and after simulated function. Int J Prosthodont 1993;6(5):435-9.

국문초록

내측연결형 임플란트에서 반복하중에 따른 지대주의 수직침하현상: 선형혼합모형 분석

서울대학교 대학원 치의과학과 치과보철학 전공

(지도교수 허 성 주)

설 현 우

연구목적 : 본 연구의 목적은 내측연결형 임플란트-지대주 연결체에 반복하중을 부여하였을 때 나타나는 수직 침하현상을 분석하고, 수직침하가 더 이상 일어나지 않는 특정 지점을 알아내고자 하는 것이다.

재료 및 방법 : 외측연결형 임플란트와 내측연결형 임플란트에 세 종류의 시멘트유지형 지대주를 각각 장착하였다. 각 임플란트와 지대주는 동일한 회사(Warantec Co., Seoul, Korea)의 제품인, 외측연결형 지대주(Ext 그룹, Hexplant®와 Straight abutment®), 내측연결형 1-piece 지대주(Int-1 그룹, Inplant®와 non-octagonal Top abutment®), 내측연결형 2-piece 지대주(Int-2 그룹, Inplant®와 octagonal Top abutment®)를 사용하였으며, 각 그룹마다 7개의 시편을 준비하였다. 반복하중을 부여하기 전에, 반복체결에 따른 수직침하량을 측정하기 위하여, 임플란트-지대주 연결체를 각각 5 Ncm와 30 Ncm으로 체결한 상태에서의 길이변화량을 측정하였다. 이후 반복하중 전과

후에 각각 Periotest® 값(PTV)과 풀림토크값(RTV)을 측정하여 임플란트-지대주 연결부위의 안정성을 평가하였다. 임플란트-지대주 연결체에 수직하중을 적용하기 위하여 임플란트 받침대에 고정한 상태에서, 3 Hz 및 150 N의 조건으로 백만 회의 반복하중을 부여하였다. 수직침하량은 0, 10, 100, 1,000, 10,000, 100,000, 500,000, 1,000,000회의 반복하중 마다 각각의 길이변화량으로 측정하였다. 반복측정분산분석(RM-ANOVA)를 이용하여 반복하중의 영향을 분석하였으며, 패턴변화를 관찰하기 위하여 선형혼합모형(linear mixed model)을 사용하였다. 유의수준은 5%로 설정하였다. 반복하중 분석이 끝난 각 그룹의 1개의 시편은 미세전산화단층촬영술(micro-CT)을 통해서 내부구조를 촬영하였으며, 전자주사현미경(SEM)을 통해서 임플란트-지대주 연결부위의 표면을 평가하였다.

결과 : 반복체결에 따른 수직침하량은 Ext 그룹에서 4.0 ± 1.41 μm, Int-1 그룹에서 31.1 ± 9.48 μm, Int-2 그룹에서 48.3 ± 8.44 μm를 나타내었다. 반복하중 전에 각 그룹간의 PTV는 차이가 없었으나 반복하중 후에는 Int-2 그룹에서 유의하게 낮은 값을 나타내었으며, 각 그룹별 전후 비교에서 Int-2 그룹에서 유의하게 감소하였다. RTV의 경우, 반복하중 전에는 Int-2 그룹이 유의하게 높은 RTV값을 보였으며, 반복하중 후에는 Int-2 그룹에서 유의하게 낮은 RTV값을 보였다. 모든 그룹에서 RTV가 감소하였다. 백만 회의 반복하중에 따른 수직침하량은, Ext 그룹에서 0.6 ± 0.54 μm, Int-1그룹에서 3.7 ± 0.76 μm, Int-2 그룹에서 9.0 ± 2.38 μm를 나타내었다.

선형혼합모형을 이용한 수직침하량의 패턴분석에서는, 반복하중 171회에서 기울기의 변화가 관찰되었다. Ext그룹에서는 이 지점 (변곡점, 반복하중 171회째)의 전과 후 모두 수직침하현상이 관찰되지 않았다. Int-1 그룹에서는 변

곡점 이전에는 수직침하현상이 관찰되었으나, 이후에는 수직침하현상이 관찰되지 않았다. Int-2 그룹에서는 변곡점 전후로 모두 지속적인 수직침하가 관찰되었으나, 변곡점이 지난 이후의 기울기는 매우 완만하였다.

결론 : 이번 실험을 통하여 다음과 같은 결론을 얻었다.

1. 모든 그룹에서 체결토크에 따른 수직침하가 발생하였다.
2. 모든 그룹에서 반복하중 후 임플란트-지대주 연결부위 표면에 마모가 관찰되었다.
3. 모든 그룹에서 반복하중 후 Periotest® 값은 안정된 값을 보였으나, 풀림토크 값은 감소하였다.
4. 선형혼합모형을 이용한 분석결과, Ext 그룹 및 Int-1 그룹에서 초기에 plateau가 관찰되었다. Int-2 그룹에서는 명확한 plateau 지점을 찾기가 어려웠으나 10만회 이후에 수직침하 변화량이 완화되었다.

이번 연구를 통해 수직침하의 패턴을 분석하였으며, 풀림토크값이 감소한 것을 확인하였다. 임상에 적용함에 있어 나사풀림과 보철과정의 오차를 줄이기 위해 최소 한달 이후에 나사를 재체결하는 것이 추천된다.

주요어 : 수직침하, 선형혼합모형, 침하현상, 반복하중, 내측연결구조, 임플란트-지대주 디자인

학 번 : 2010-31197

감사의 글

박사과정을 무사히 마치고 이 논문을 시작하여 마무리하기까지 많은 도움을 주신 여러 스승님과 동료, 가족에게 감사의 말씀을 전합니다.

치과보철과 수련 및 대학원 생활에 있어 깊은 충고와 조언으로 진료와 연구에 귀중한 가르침을 주신 허성주 교수님께 깊은 감사를 드립니다. 병원 진료와 업무로 바쁘신 와중에도 본 논문을 위하여 많은 지도 편달을 해주셨습니다.

국소의치학이라는 학문의 깊이와 열정을 일깨워주시고, 이번 논문 심사에도 열과 성을 다해주신 곽재영 교수님과 김성균 교수님께도 깊은 감사를 드립니다.

바쁘신 와중에도 본 논문 심사를 위해서 꼼꼼히 살펴주신 치과생체재료학교실의 임범순 교수님과 연세대학교 치과대학의 한동후 교수님께도 감사드립니다.

항상 격려와 조언을 아끼지 않으신 치과보철학교실의 이재봉 교수님, 한중석 교수님, 임영준 교수님, 김성훈 교수님, 김명주 교수님, 권호범 교수님, 여인성 교수님과 치과보철학교실원 여러분께 이 자리를 빌어 감사의 말씀을 전합니다.

치과보철과 수련기간부터 지금까지 항상 동고동락하며 서로를 격려해 준 동기들과 의국 선후배님들에게도 감사의 말씀을 전합니다.

오늘의 제가 있기까지 많은 사랑과 정성으로 보살펴주시고 지원해주신 부모님께 깊은 감사를 드리며, 제가 하는 모든 일을 응원해주시는 장인, 장모님께도 깊은 감사를 드립니다.

마지막으로, 치과대학과 수련생활, 대학원생활을 지금까지 묵묵히 함께해준 영원한 친구이자 인생의 반려자인 사랑하는 아내와 제 인생에 있어 크나큰 선물인 지훈과 지효에게 고마움을 전합니다.

2013년 12월

설 현 우